

1 Title Page

2

3 **Exploring the use of otolith shape analysis to identify the stock spatial structure**
4 **of dusky rockfish (*Sebastes variabilis*)**

5

6 Todd T. TenBrink¹, Jane Y. Sullivan², and Christopher M. Gburski¹

7

8 ¹National Oceanic Atmospheric Administration, National Marine Fisheries Service, Alaska
9 Fisheries Science Center, 7600 Sand Point Way NE, Seattle WA 98115 USA

10 ²National Oceanic Atmospheric Administration, National Marine Fisheries Service, Alaska
11 Fisheries Science Center, 17109 Point Lena Loop Road, Juneau AK 99801 USA

12

13 Corresponding author's email: todd.tenbrink@noaa.gov

14

15

16

17

18

19

20

21

22

23 **Abstract**

24 Dusky rockfish (*Sebastes variabilis*) is a commercially valuable groundfish species in Alaska
25 waters, with its highest abundance and fishery catch occurring in the Gulf of Alaska (GOA), and
26 lesser abundance and catch occurring throughout the Aleutian Islands and southeastern Bering
27 Sea. Despite its commercial importance, information regarding stock structure of dusky rockfish
28 has been data-limited. In this study, otolith shape analysis was used to evaluate the stock
29 structure of dusky rockfish across five geographical subareas exhibiting ecological differences in
30 the GOA and Bering Sea and Aleutian Islands (BSAI), where dusky rockfish are managed as two
31 separate stocks. A combination of size and shape indices, wavelet and elliptic Fourier
32 descriptors, were examined from left and right-side otoliths collected from these regions ($n =$
33 522). Individual variation existed across subareas. Wavelet and elliptic Fourier descriptors
34 indicated that mean otolith shapes were partitioned between the two management regions but
35 also showed a high degree of overlap among subareas. Classification accuracies of otoliths to
36 their subarea of origin through linear discriminant analysis (LDA) were variable (6.3% to 73.5%
37 and 15.4% to 65.8% correctly classified for the elliptic Fourier and wavelet analyses,
38 respectively). The highest classification rates were found between the western GOA and
39 eastern Aleutian Islands, contributing to the observed differences between management
40 regions and providing some support for current management paradigms. Dusky rockfish
41 exhibited low to moderate overall classification rates (43.9% to 52.2%), suggesting minimal
42 stock structure within Alaska waters. This study highlights the utility of otolith shape analysis as
43 a stock discrimination tool, and results will help refine further investigations and support
44 fishery management in Alaska.

45 **Keywords:** Dusky rockfish, *Sebastes*, otolith shape analysis, population structure, stock
46 assessment

47

48 **1. Introduction**

49 Knowledge of stock structure is critical to understanding population biology and dynamics, and
50 is necessary for effective sustainable fisheries management. According to Hilborn and Walters
51 (1992), stocks are defined as homogenous populations of fish, with individuals of these
52 populations having similar life history characteristics. However, while the appropriate definition
53 of a stock has remained a challenge to management (Cadrin et al., 2014), its concept remains
54 fundamental to stock assessment and fisheries management. Implementing appropriate stock
55 structure and spatial extent within assessments and fisheries management can, at least in
56 principle, sustain productive fisheries, whereas ignoring or misspecifying stock structure can
57 have potentially deleterious effects, including overfishing or failure to detect declines in a latent
58 population (see Cadrin, 2020 for a review of case studies and best practices). Identifying the
59 appropriate stock structure draws from a suite of complementary, interdisciplinary techniques
60 that cover multiple aspects of the life history characteristics of a fish species, which includes
61 addressing both genetic and phenotypic variation (Begg et al., 1999).

62

63 Otolith shape analysis has been used globally to discriminate stocks or identify stock structure
64 for a variety of marine fish to inform management (Campana and Casselman, 1993), including
65 mulloway (*Argyrosomus japonicas*; Ferguson et al., 2011); anglerfish (*Lophius piscatorius*; Cañas
66 et al., 2012); European anchovy, *Engraulis encrasicolus*; Bacha et al., 2014); Patagonian

67 toothfish (*Dissostichus eleginoides*; Lee et al., 2018); blue jack mackerel, (*Trachurus picturatus*;
68 Moreira et al., 2019); and European hake (*Merluccius merluccius*; Moralis-Nin et al., 2022). For
69 rockfishes (*Sebastes* spp.), otolith shape and morphometric analysis has been conducted for
70 commercially important species across their range. Otolith shape analysis involves a
71 quantitative geometric description using methods such as elliptic Fourier analysis of two-
72 dimensional otolith shapes (Lestrel, 1997), thus capturing biological information that can be
73 compared between populations within or between species. Use of basic external indices that
74 describe the otolith size or shape have been used in combination with these more complex
75 analyses to identify stock structure of commercially important species (Ferguson et al., 2011;
76 Mapp et al., 2017; Mahê et al., 2019; Moreira et al., 2019). In the northwest and northeast
77 Pacific Ocean, these studies have demonstrated the importance and utility of using otolith
78 shape among rockfishes to distinguish between species (Zhuang et al., 2015; Park et al., 2023);
79 to identify patterns of otolith shape from sympatric species to correlate morpho-types with
80 ecological traits (Tuset et al., 2015); and to indicate differences between potential nearshore
81 and offshore stocks (Vaux et al., 2019).

82

83 Dusky rockfish (*Sebastes variabilis*) is a commercially valuable rockfish found along and in outer
84 continental shelf waters of Alaska (Williams et al., 2022). The highest abundances occur in the
85 Gulf of Alaska (GOA), with the largest biomass estimates reported in the western GOA (von
86 Szalay and Raring, 2018; Fig. 1). In the GOA, where dusky rockfish is part of a targeted rockfish
87 (*Sebastes* spp.) trawl fishery and assessed through statistical catch-at-age modeling, fishery
88 catches have remained below acceptable biological catches (ABCs) and overfishing levels (OFLs);

89 Williams et al., 2022). Dusky rockfish abundance is considerably lower in the Bering Sea and
90 Aleutian Islands management region (BSAI), where it is assessed as part of a non-target, and
91 comparatively data-poor multispecies rockfish complex using index-based methods (Sullivan et
92 al., 2022). Dusky rockfish primarily occur in the Aleutian Islands within the BSAI management
93 region and are rarely observed in the eastern Bering Sea (Hoff, 2016; Markowitz et al., 2022;
94 Fig. 1). The biology of dusky rockfish is data-limited, although recent work showed that size
95 structure and growth between sexes exhibited homogeneity across the Aleutian Islands
96 (TenBrink et al., 2023). In the GOA, life history traits of dusky rockfish have been more broadly
97 studied, but data gaps persist, including information on the spatial and temporal extent of
98 these traits (Malecha et al., 2007; Williams et al., 2022).

99

100 Within the BSAI management region, dusky rockfish catch is the largest of any species within its
101 multispecies rockfish complex (361 metric tons; approximately 60% of complex in 2021; Sullivan
102 et al., 2022), even exceeding catches of shortspine thornyhead (*Sebastolobus alascanus*), which
103 comprises approximately 95% of the stock complex's total estimated biomass. Dusky rockfish
104 are primarily caught in the Atka mackerel (*Pleurogrammus monoptygius*) bottom trawl
105 fishery. In recent years, high exploitation rates (catch/biomass) in the eastern Aleutian Islands
106 (Sullivan et al., 2022; Fig. 1) have prompted concerns about localized depletion (Hanselman et
107 al., 2007) and highlighted data gaps on dusky rockfish stock structure in Alaska waters (Lunsford
108 et al., 2011). In addition, within the federal management range of dusky rockfish in Alaska,
109 there are distinct ecological boundaries that exist. In the BSAI region, the Aleutian Islands is
110 divided by eastern, central, and western ecoregions within this marine ecosystem (Ortiz and

111 Zador, 2021). The western GOA is a large coastal ocean system dominated by the Alaska Coastal
112 Current, while the eastern GOA has a narrow continental shelf influenced by the northward-
113 flowing Alaska Current (Stabeno et al., 2004). An ecological boundary has been found near
114 148°W in the GOA (Coffin and Mueter, 2016; Fig. 1). We therefore undertook an otolith shape
115 analysis study to identify dusky rockfish stock structure throughout its range in two bordering
116 management regions. The objectives of our study were to 1) use otolith shape analysis to
117 determine if there are differences in otolith shape between management regions using two
118 descriptor techniques, and 2) to test for differences in otolith shape among subareas of each
119 management region that exhibit ecological and oceanographic differences.

120

121 **2. Material and methods**

122 *2.1 Study area and sampling*

123 A total of 522 paired sagittal otoliths from dusky rockfish specimens were collected from both
124 fisheries-dependent and fisheries-independent sampling platforms with bottom trawl gear
125 during 2019-2022 (Table 1). The fork length and weight of each dusky rockfish specimen was
126 measured to the nearest centimeter and gram, respectively. The sex of each fish was
127 determined by gonadal examination. Left and right otoliths were collected and stored in a 50%
128 glycerol thymol solution prior to processing. Otoliths were collected across the GOA and BSAI
129 management regions (Fig. 1). Spatial reconstruction of the study area was created through the
130 R package “sf” (Pebesma, 2018; Pebesma and Bivand, 2023) and “ggplot2” (Wickham, 2016).
131 Subareas within each region follow the numerical statistical areas associated with the GOA and
132 BSAI fishery management plans (North Pacific Fishery Management Council; NPFMC, 2020a;

133 NPFMC, 2020b). From bottom trawl research surveys conducted by the National Marine
134 Fisheries Service's Alaska Fisheries Science Center in the summer, the BSAI sampling occurred
135 on the continental shelf and upper continental slope to a depth of 500 m from Attu Island in the
136 west to Unimak Island in the east (Fig. 1; von Szalay and Raring, 2020). From the BSAI
137 management region, otoliths were collected across the Aleutian Islands. The survey samples in
138 multiple regions that exhibit distinct oceanographic and biological characteristics. The three
139 Aleutian Islands ecoregions also encompass primary management or statistical subareas (Fig.
140 1). We define subareas for this study as western Aleutian Islands (WAI; 543), central Aleutian
141 Islands (CAI; 542), and eastern Aleutian Islands (EAI; 541) that follow the aforementioned
142 management areas. The GOA bottom trawl survey covered the continental shelf and upper
143 continental slope to 700 m from the Islands of the Four Mountains to the west and east to
144 Dixon Entrance (Fig. 1; von Szalay and Raring, 2018). Among the two GOA ecological divisions,
145 there are five management statistical areas. In this study, we define our subareas in the GOA as
146 western GOA (WGOA; 610, 620, 630) and eastern GOA (EGOA; 640 and 650). Fish were also
147 sampled by fishery observers during Atka mackerel and rockfish bottom trawl fisheries in the
148 GOA and BSAI throughout the calendar year.

149

150 *2.2 Otolith image acquisition and processing*

151 Undamaged otoliths were blotted dry and placed on a black surface with the sulcus facing
152 downward and the rostrum (anterior) end pointing to the left. Under reflected light, a
153 calibrated high-resolution image of the proximal face of either the left or right sagittal otolith
154 from either sex was obtained with a digital microscope camera (Leica DMC4500) mounted on a

155 Leica stereo microscope MZ9.5. During this process a fixed, single magnification of 6.3× was
156 used (10x eyepieces; 0.63x zoom; 1.0x main objective). Before shape analysis, each otolith
157 image was edited to show the maximum amount of contrast between the otolith and
158 background. Adobe Photoshop Elements version 18.0 was used to contrast the white otoliths
159 with the black background, if necessary. Subsequent measurements were based on these
160 captured images. Images of left and right-side otoliths were analyzed separately in this study.
161 Few samples of right-side otoliths were collected from subarea WAI; therefore, right-side
162 otoliths from the WAI were not included in subsequent analysis.

163

164 *2.3 Otolith shape analysis*

165 Otolith shape analysis was performed using the “shapeR” package (Libungan and Palsson, 2015)
166 in R version 4.2.2 (R Core Team, 2022). In “shapeR”, the original jpeg-formatted images of each
167 otolith were transformed into gray-scale and the outlines were detected using a threshold pixel
168 value of 0.2. Each digitized image was visually evaluated to ensure that each outline accurately
169 captured the edge of the otolith. If the digitized outline did not closely match the otolith outline
170 (e.g., due to high pixel noise), the original image was manually edited and digitization was
171 repeated. Contour smoothing was also performed (Libungan and Palsson, 2015).

172

173 Two types of otolith shape descriptors were used from the otolith outlines: wavelet and elliptic
174 Fourier (Libungan and Palsson, 2015). Both descriptors were chosen due to their reported
175 differences in performance when describing stock structure of fish species (e.g., Neves et al.,
176 2023). Reconstruction of the otolith shape using wavelet and elliptic Fourier descriptors were

177 generated and standardized with fish fork length to minimize ontogenetic effects (Libungan and
178 Palsson, 2015). The level of wavelet and number of Fourier harmonics needed for a 98.5%
179 accuracy of the otolith outline reconstruction was 5 and 12, respectively. In order to further
180 minimize ontogenetic effects, samples were truncated to 38-50 cm fork length. This size range
181 encompassed adult, mature fish captured from similar depth profiles. Wavelet and elliptic
182 Fourier descriptors produced 64 and 45 standardized coefficients, respectively. Coefficients that
183 had a significant interaction with fork length ($P < 0.05$) were excluded from analysis. The
184 remaining standardized coefficients were used to compare otolith shape among subareas using
185 canonical analysis of principal coordinates (CAP).

186

187 Four primary indices related to the size of the otolith were used (area, perimeter, otolith
188 length, and otolith width; Fig. 2). Otolith weight was added as an index to account for
189 differences in otolith characteristics such as thickness. From the primary size indices, six shape
190 indices were calculated to determine if otolith shape varied among subareas within the GOA
191 and BSAI management regions (Table 2). Data were standardized using fork length for each
192 specimen as size effects can bias stock structure (Smith, 1992) using the common within-group
193 slope (Lombarte and Leonart, 1993),

194

$$195 \quad M_S = M_O \left(\frac{x}{x} \right)^b$$

196 where,

197 M_S = standardized (size-adjusted) measurement.

198 M_O = original parameter (size or shape index).

199 \underline{x} = average size parameter (fork length) for all datasets.

200 x = size parameter (fork length) of each fish species.

201 b = slope of the regression between $\log M_0$ and $\log x$.

202

203 The standardized size and shape indices were evaluated for normality and homogeneity of
204 variance. The data deviated from a normal distribution (Shapiro-Wilks test of normality, $P <$
205 0.025) and equality of variances across areas (Levene's test, $P < 0.001$); therefore, non-
206 parametric tests were used for comparison analysis. The calculated shape indices were
207 evaluated for collinearity using Pearson correlation coefficients, with a minimum value of ± 0.70
208 exhibiting significance between indices (Dormann et al., 2013). Roundness, ellipticity, and
209 aspect ratio were all highly positively correlated (≥ 0.85), and form factor was positively
210 correlated with circularity (≥ 0.95); therefore, only circularity, rectangularity, and roundness
211 were retained for analysis.

212

213 *2.5 Statistical analysis*

214 A combination of univariate and multivariate analyses was used to describe otolith shape in this
215 study. Non-parametric Kruskal-Wallis tests were used to test otolith shape between subareas
216 for each size and shape index ("rstatix" R package; Kassambara, 2023). The eta-squared (η^2),
217 based on the Kruskal-Wallis H -statistic, was used as a measure of the otolith shape effect size.
218 Interpreting η^2 effect values followed Cohen (1988): $0.01 - 0.06$ (small effect), $0.06 - 0.14$
219 (moderate effect), and ≥ 0.14 (large effect). Welch t-tests were applied to each size and shape
220 index to compare their overall means between the GOA and BSAI management regions. For

221 multivariate analyses, the otolith shape variation was visualized and compared with a CAP on
222 the standardized wavelet and elliptic Fourier coefficients using the “vegan” R package (Oksanen
223 et al., 2013). ANOVA-like permutation tests of the standardized coefficients were used to
224 examine the differences in otolith shapes from each subarea based on 1,000 permutations.
225 To determine whether otoliths collected in different subareas could be distinguished based on
226 their shapes (Klecka, 1980), a linear discriminant analysis (LDA) was applied to the standardized
227 wavelet and elliptic Fourier coefficients (Libungan and Palsson, 2015). LDA is a supervised
228 dimensionality reduction and data classification procedure and was conducted using the *lda*
229 function within the “MASS” R package (Venables and Ripley, 2002) and PAST statistics software
230 (ver. 3.19; Hammer et al., 2001). Predictive models were examined for accuracy using
231 jackknifed cross-validation (‘leave-one-out’), which calculates an unbiased estimation of
232 classification success. LDA was performed on different models that compared the performance
233 of the standardized wavelet and elliptic Fourier coefficients and shape indices. A one-way
234 permutational multivariate analysis of variance (PERMANOVA) was used to statistically test
235 differences among subareas. PERMANOVA dissimilarity matrices were based on Euclidean
236 distance and Type III (partial) sum of squares, and calculated using 9,999 random permutations
237 (Anderson, 2005).

238

239 **Results**

240 3.1 *Otolith morphometric analysis*

241 The mean values for the standardized size and shape indices varied across subareas for both
242 left-side and right-side otoliths (Fig. 3). With the exception of circularity, all size and shape

243 indices were different among some subareas ($P < 0.05$; Kruskal-Wallis; Fig. 3). For the right-side,
244 otolith area had the largest shape effect (Table 3), with those from the EGOA being the largest.
245 Mean otolith length and mean otolith weight also exhibited moderate to large effects among
246 right-side otoliths (Fig. 3). For left-side otoliths, roundness exhibited the largest effect, with
247 those from subareas of the Aleutian Islands having the highest mean values, and those otoliths
248 from the EGOA and WGOA having the lowest (Fig. 3). Mean otolith length, otolith width, and
249 roundness from left-side otoliths, and mean otolith length and roundness from right-side
250 otoliths were significantly different between the BSAI and GOA management regions (Welch t-
251 tests; $P < 0.05$).

252

253 3.2 Otolith shape analysis

254 Outline reconstruction of the mean shape of otoliths using both standardized wavelet and
255 Fourier coefficients were similar for each otolith side. For the left-side otolith, two main
256 sections were identified where divergences occurred among subareas (Fig. 4A; Supplementary
257 Fig. S1). These divergences were observed along the otolith rostrum and posterior side of the
258 otolith. Among these sections, the mean otolith shape had the strongest variation at an angle
259 approximately between 0° - 45° and from this 300° - 360° angle range. The mean otolith shapes of
260 right-side otoliths showed divergences along the rostrum near 180° and the posterior ventral
261 edge between -300° - 360° (Fig. 4B; Supplementary Fig. S1). ANOVA-like permutations tests
262 showed significant differences in the mean otolith shape of dusky rockfish between subareas
263 from wavelet and elliptic Fourier coefficients among left and right-side otoliths ($P < 0.001$; Table
264 4).

265

266 CAP plots showed heterogeneity among the subareas with some distinction among
267 management regions (Fig. 5). For left-side otoliths, the first two axes explained > 85% of the
268 variation using wavelet and elliptic Fourier coefficients (Fig. 5). There was a high degree of
269 overlap among otolith shapes, with variability in individual otoliths across subareas. A general
270 ordination pattern was evident along the first canonical axis, showing two different cluster
271 groups (WAI, CAI, and EAI; and WGOA and EGOA). Right-side otoliths exhibited a similar
272 ordination pattern along the first canonical axis (Fig. 5).

273

274 Classification from jackknifed LDA showed an overall success of 45.6% and 52.2% for Fourier
275 descriptors for the left-side and right-side otoliths, respectively (Fig. 6A, B). Wavelet descriptors
276 exhibited similar results for each otolith side, but the success rate was slightly lower
277 (Supplementary Fig. S2). Use of only shape indices performed poorly, with left and right-side
278 otoliths exhibiting classification success of 34.5% and 24.8%, respectively (Supplementary Fig.
279 S3). Both shape descriptors showed the highest classification rates in the WGOA and the EAI.
280 Classification success was generally poor across the periphery of the study range in the WAI and
281 EGOA for left-side otoliths (Fig. 6A), and correctly classified only 30.8% in the CAI for right-side
282 otoliths (Fig. 6B). PERMANOVA pairwise tests revealed statistically significant differences
283 between all subareas for right-side otoliths, with the exception of otoliths collected in CAI and
284 EAI using Fourier descriptors (Table 5). There were also no differences observed for EGOA and
285 WGOA using wavelet descriptors. PERMANOVA tests for left-side otoliths exhibited a general
286 pattern of significant differences between otolith shape between management regions.

287

288 **Discussion**

289 What was previously known about dusky rockfish stock structure was based on an evaluation of
290 known biological information by Lunsford et al. (2011), which included compiling available data
291 from survey and fishery sources on life history, habitat, oceanography, distribution and
292 population trends from the GOA. This prior study determined that dusky rockfish exhibited
293 minimal stock structure. However, major deficiencies in the aforementioned data were noted,
294 including any temporal or spatial study that determined if the dusky rockfish population was a
295 single stock. The most recent stock assessment of dusky rockfish in the GOA continues to
296 support a minimum stock structure hypothesis based on this previous information, but further
297 research was deemed necessary to help evaluate this (Williams et al., 2022). For dusky rockfish
298 in the BSAI management region, there has been a complete absence of information to
299 determine stock structure (Sullivan et al., 2022); however, conservation concerns related to
300 relatively high incidental catches of dusky rockfish in the Atka mackerel fishery in the eastern
301 Aleutian Islands have prompted a need for further research into dusky rockfish stock structure
302 in Alaska waters.

303

304 This was the first study that investigated otolith morphometry and shape analysis as
305 discrimination tools to characterize stock structure for dusky rockfish across its range in Alaska.
306 Our results indicated that otoliths from individual dusky rockfish were highly variable but
307 differences were found in univariate measurements and mean otolith shape between
308 management regions and, in some instances, among subareas. CAP results indicated a high

309 degree of overlap among otolith shapes among subareas; however, a general ordination
310 pattern was evident along the first canonical axis, with subareas clustered by management
311 region (Fig. 5). These patterns were consistent between right and left-side otoliths and between
312 the elliptic Fourier and wavelet shape descriptors (Fig. 5). The LDA of mean otolith shape
313 indicated some separation between subareas. The highest classification rates for both elliptic
314 Fourier and wavelet shape descriptors were observed in the WGOA and the EAI, whereas
315 classification success was generally poor across the periphery of the study range in the WAI and
316 EGOA (Fig. 6). Based on otolith shape analysis, our results appear to support the current fishery
317 management paradigm of separate dusky rockfish stocks in the GOA and BSAI with overall low
318 to moderate stock structure throughout Alaska waters.

319
320 Otolith shape analysis involving contour reconstruction provides a more complex knowledge on
321 otolith shape variability (Tuset et al., 2021), but the use of size or shape indices in this study
322 was not necessarily limited. Of the two shape descriptors, elliptic Fourier achieved slightly
323 better results than wavelet. Differences between the two descriptors have been noted (e.g.,
324 Graps, 1995; Libungan and Palsson, 2015), and both were useful in discriminating among
325 subareas. There have been few studies that compared both routinely-used descriptors (e.g.,
326 Neves et al., 2023), but our results agree with Sadighzadeh et al. (2012), who suggested that
327 the elliptic Fourier descriptor is more efficient in describing variation within species. In the
328 future, additional tools and methods to assess classification performance using Fourier analysis,
329 such as machine-learning techniques (Smolinski et al., 2020) and combining geographical areas
330 (Stransky, 2005), could improve accuracy.

331

332 The stock structure of dusky rockfish indicated by otolith shape analysis appears to be similar to
333 that derived from other sets of life history traits (i.e, growth). Campana and Casselman (1993)
334 concluded that otolith shape was strongly related to fish growth rate, and, consequently, that
335 otolith shape might not differentiate well among stocks with similar growth rates. Growth of
336 dusky rockfish in Alaska has not been studied extensively. Spatial variation has been reported,
337 as Malecha et al. (2007) found significant differences in growth between areas in the GOA, but
338 issues with sample sizes were noted from the eastern GOA. In the current stock assessment of
339 dusky rockfish in the GOA, growth within the age-structured model is combined for both sexes
340 and area (Williams et al., 2022). In the Aleutian Islands, TenBrink et al. (2023) found no
341 differences in growth among samples collected across the eastern, central, and western
342 subareas. Sexual dimorphism among otolith shape should be investigated further in dusky
343 rockfish; however, as Vaux et al. (2019) found secondary sexual differences in otolith shape in
344 deacon rockfish (*Sebastes diaconus*). A robust study on dusky rockfish growth rates and
345 subsequent examination of sexual differences among otolith shape across its longitudinal range
346 might help further detect spatial similarities or differences.

347

348 Differences in otolith shape has been linked to genetic (Vignon and Morat, 2010) and
349 environmental effects, such as temperature (Lombart and Lleonart, 1993) and diet (Mille et al.,
350 2016), which would affect the growth phase across sizes of fish. In our study, sampled across a
351 very large area, regional environmental differences exist. For example, Samalga Pass in the
352 Aleutian Islands, directly east of the Islands of the Four Mountains near the management

353 border of subareas EAI and WGOA (Fig. 1), is a well-documented oceanographic barrier that
354 separates the warmer, fresher, nitrate-poor water in the GOA from the colder, saltier, and
355 nitrate-rich water of the Aleutian Islands (Ladd et al., 2005; Zimmerman and Prescott, 2021).
356 Hunt and Stabeno (2005) described a strong discontinuity in the marine ecosystem east and
357 west of Samalga Pass, including differences in the species composition of zooplankton, cold-
358 water corals, groundfish, seabirds, and marine mammals. The oceanographic barrier at Samalga
359 Pass may explain the higher classification rates in the WGOA and EAI. Several other large passes
360 throughout the Aleutian Islands (Zimmerman and Prescott, 2021) may further isolate dusky
361 rockfish within localized areas (e.g., subareas CAI and WAI), and a finer-scale spatial analysis of
362 the data presented in this study could be used to analyze these patterns. In the GOA,
363 spatiotemporal variation in the timing and magnitude of chlorophyll-a concentrations related to
364 sea surface temperature, freshwater discharge, and other oceanographic variables (Waite and
365 Mueter, 2013) may result in differential prey availability for dusky rockfish among subareas in
366 that management region. A delineation near 148°W in the GOA separating eastern and western
367 areas is created by two distinct downwelling regions (Coffin and Mueter, 2016). Behrenfeld and
368 Falkowski (1997) found that carbon (¹⁴C) productivity also shows regional boundaries between
369 the two areas. Further research and increased sample sizes would be needed to test the
370 hypothesis that otolith shape could be an indicator allowing the characterization of populations
371 of dusky rockfish between areas with different ecological conditions.

372

373 All rockfish stocks in the U.S. Exclusive Economic Zone off Alaska, including Pacific ocean perch
374 (*S. alutus*), northern (*S. polyspinis*), rougheye (*S. aleutianus*), blackspotted (*S. melanostictus*),

375 and shortraker rockfish (*S. borealis*), are managed as separate stocks within single and multi-
376 species assessments in the GOA and BSAI. However, data to support this separation are limited,
377 and otolith shape analysis offers a promising, low cost method of stock delineation that could
378 support management of many of these rockfish stocks. For example, high exploitation rates of
379 blackspotted and rougheye rockfish in the western Aleutian Islands have prompted questions
380 about stock structure and spatial management in that region (Spencer et al., 2010; Spencer et
381 al., 2022). While preliminary results from a low coverage whole genome sequencing analysis
382 suggest a lack of population genetic structure for blackspotted and rougheye rockfish in the
383 Aleutian Islands, persistent low abundance coupled with increasing exploitation rates warrant
384 further examination (Larson et al., 2021). Application of otolith shape analysis could provide
385 additional information on demographic connectivity for this stock, which may have more
386 relevance to fisheries management than genetic structure (Waples et al., 2008).

387

388 Defining stock structure is a critical piece in management decision making. The lack of defining
389 spatial structure in stock assessment models may lead to misperceptions of stock status
390 (Cadrin, 2020), eventually leading to erroneous management reference points that have failed
391 to capture the spatial component when evaluating stocks in model development. Given that
392 some degree of partitioning was observed in our multivariate analysis, this otolith shape
393 analysis provides some support for existing fisheries management of dusky rockfish in Alaska,
394 which separates catch recommendations between the GOA and BSAI (Sullivan et al., 2022;
395 Williams et al., 2022). The subareas with the highest catches and biomass in each management
396 region (subarea 541 in the EAI and subareas 630, 620, and 610 in the WGOA) have a low to

397 moderate level of population connectivity, with a relatively high number of samples being
398 classified in the other subarea if not correctly classified. If dusky rockfish in these subareas are
399 connected, either through larval dispersal or adult migration, this could imply reduced
400 management concern for subareas like EAI with high exploitation rates. However, given the
401 mixed results of this study and the need to disentangle suspected sources of variation such as
402 sex, sampling year, and associated spatial ecological differences, further analysis of dusky
403 rockfish demographic rates, including movement patterns, habitat utilization (e.g., Conrath et
404 al., 2019), and size and age structure, is warranted. Additional procedures, such as genomics or
405 genetics (Vignon and Morat, 2010; Rodgveller et al., 2017; Vaux et al., 2019), body morphology
406 (Düranni et al., 2022), and otolith elemental chemistry (Ferguson et al., 2011) would provide a
407 more thorough understanding of dusky rockfish stock structure.

408

409 **Credit author contribution statement**

410 **T. T. TenBrink** – Conceptualization, Methodology, Data curation, Formal analysis, Investigation,
411 Writing, Visualization, Project Administration; **J. Y. Sullivan** – Methodology, Investigation,
412 Writing, Visualization; **C. M. Gburski** – Data curation, Methodology, Visualization, Writing.

413

414 **Acknowledgments**

415 Comments from Cara Rodgveller and Kristen Omori improved earlier versions of the
416 manuscript. Additionally, comments provided by three anonymous reviewers and the Editor
417 were greatly appreciated. The findings and conclusions in this paper are those of the authors

418 and do not necessarily represent the views of the National Marine Fisheries Service. Reference
419 to trade names does not imply endorsement by the National Marine Fisheries Service, NOAA.

420

421 **Funding**

422 This research did not receive any specific grant from funding agencies in the public, commercial,
423 or not-for-profit sectors.

424

425 **References**

426 Anderson, M.J., 2005. Permutational multivariate analysis of variance. *Dep. Stat., Univ. Auckl.*,
427 *Auckl.*, 26, 32-46.

428

429 Bacha, M., Jemaa, S., Hamitouche, A., Rabhi, K., Amara, R., 2014. Population structure of the
430 European anchovy, *Engraulis encrasicolus*, in the SW Mediterranean Sea, and the Atlantic
431 Ocean: evidence from otolith shape analysis. *ICES J. Mar. Sci.* 110, 2429-2435.

432 <https://doi.org/10.1093/icesjms/fss006>.

433

434 Behrenfeld, M. J., Falkowski, P. G., 1997. Photosynthetic rates derived from satellite-based
435 chlorophyll concentration. *Limnol. Oceanogr.* 42, 1–20.

436

437 Cadrin, S. X., Kerr, L. A., Mariani, S. (Eds.), 2014. *Stock Identification Methods: Applications in*
438 *Fisheries Science*, 2nd ed. Elsevier Academic Press, 566 p.

439

440 Cadrin, S. X., 2020. Defining spatial structure for fishery stock assessment. *Fish. Res.* 221,
441 105397. <https://doi.org/10.1016/j.fishres.2019.105397>.

442

443 Campana, S. E., Casselman, J. M., 1993. Stock discrimination using otolith shape-analysis. *Can. J.*
444 *Fish. Aquat. Sci.* 50, 1062-1083. <https://doi.org/10.1139/f93-123>.

445

446 Coffin, B., Mueter, F., 2016. Environmental covariates of sablefish (*Anoplopoma fimbria*) and
447 Pacific ocean perch (*Sebastes alutus*) recruitment in the Gulf of Alaska. *Deep-Sea Res. II: Top.*
448 *Stud. Oceanogr.* 132, 194–209.

449

450 Cohen, J., 1988. *Statistical Power Analysis for the Behavioral Sciences* (2nd ed.). Hillsdale, NJ:
451 Erlbaum.

452

453 Conrath, C. L., Rooper, C. N., Wilborn, R. E., Knoth, B. A., Jones, D. T., 2019. Seasonal habitat use
454 and community structure of rockfishes in the Gulf of Alaska. *Fish. Res.* 219, 105331.
455 <https://doi.org/10.1016/j.fishres.2019.105331>.

456

457 Dormann, C. F., Elith, J., Bacher, S., Buchmann, C., Carl, G., Carre, G., Marquez, J. R. G.,
458 Gruber, B., Lafourcade, B., Leitao, P. J., Münkemüller, T., McClean, C., Osborne, P. E., Reineking,
459 B., Schroder, B., Skidmore, A. K., Zurell, D., Lautenbach, S., 2013. Collinearity: a review of
460 methods to deal with it and a simulation study evaluating their performance. *Ecogr.* 36, 027–
461 046. <https://doi.org/10.1111/j.1600-0587.2012.07348.x>

462

463 Dürrani, Ö., Bal, H., Battal, Z. S., Seyhan, K., 2022. Using otolith and body shape to discriminate
464 between stocks of European anchovy (Engraulidae: *Engraulis encrasicolus*) from the Aegean,
465 Marmara and Black Seas. J. Fish. Biol. 101, 1452-1465. <https://doi.org/10.1111/jfb.15216>.

466

467 Ferguson, G. J., Ward, T. M., Gillanders, B. M., 2011. Otolith shape and elemental composition:
468 Complementary tools for stock discrimination of mulloway (*Argyrosomus japonicus*) in southern
469 Australia. Fish. Res. 110, 75-83. <https://doi.org/10.1016/j.fishres.2011.03.014>.

470

471 Graps, A., 1995. An Introduction to Wavelets. IEEE Comp. Sci. Eng. 2, 50–61.

472

473 Hammer, Ø., Harper, D. A. T., Ryan, P. D., 2001. PAST: Paleontological statistics software
474 package for education and data analysis. Palaeontol. Electron. 4, 9.

475

476 Hanselman, D., Spencer, P., Shotwell, K., Reuter, R., 2007. Localized depletion of three Alaska
477 rockfish species. In Biology, assessment, and management of North Pacific rockfishes (J. Heifetz,
478 J. DiCosimo, A. J. Gharrett, M. S. Love, V. M. O’Connell, and R. D. Stanley, eds.). Univ. Alaska Sea
479 Grant Program Report AK-SG-07-01, Fairbanks, AK., pp. 493-511.

480

481 Hoff, G. R., 2016. Results of the 2016 eastern Bering Sea upper continental slope survey of
482 groundfish and invertebrate resources. U.S. Dep. Commer., NOAA Tech. Memo. NMFS-AFSC-
483 339, 272 p.

484

485 Hunt, G. L., Stabeno, P. J., 2005. Oceanography and ecology of the Aleutian Archipelago: Spatial
486 and temporal variation. *Fish. Oceanogr.*, 14, 292–306. [https://doi.org/10.1111/j.1365-](https://doi.org/10.1111/j.1365-2419.2005.00378.x)
487 [2419.2005.00378.x](https://doi.org/10.1111/j.1365-2419.2005.00378.x)

488

489 Kassambara, A., 2023. Rstatix, ver. 7.0.2. <https://rpkgs.datanovia.com/rstatix/>.

490

491 Klecka, W. R., 1980. *Discriminant Analysis*. Beverly Hills, CA: Sage Publications.

492

493 Ladd, C., Hunt, G. L. Jr., Mordy, C. W., Salo, S. A., Stabeno, P. J., 2005. Marine environment of
494 the eastern and central Aleutian Islands. *Fish. Oceanogr.* 14, 22–38.
495 <https://doi.org/10.1111/j.1365-2419.2005.00373.x>

496

497 Larson, W., Spies, I., L. Timm., 2021. Genetic population structure of blackspotted rockfish in
498 Alaska using low coverage whole genome sequencing (lcWGS), and its management
499 implications. Prepared for the September 2021 North Pacific Fishery Management Council's
500 Groundfish Plan Team Meeting.
501 [https://meetings.npfmc.org/CommentReview/DownloadFile?p=98f3a948-e478-4b3d-b039-](https://meetings.npfmc.org/CommentReview/DownloadFile?p=98f3a948-e478-4b3d-b039-284b712332fd.pdf&fileName=Blackspotted_Genetics.pdf)
502 [284b712332fd.pdf&fileName=Blackspotted_Genetics.pdf](https://meetings.npfmc.org/CommentReview/DownloadFile?p=98f3a948-e478-4b3d-b039-284b712332fd.pdf&fileName=Blackspotted_Genetics.pdf).

503

504

505

506 Lee, B., Brewin, P. E., Brickle, P., Randhawa, R., 2018. Use of otolith shape to inform stock
507 structure in Patagonian toothfish (*Dissostichus eleginoides*) in the southwestern Atlantic. Mar.
508 Freshw. Res. 69(8), 1238-1247. <https://doi.org/10.1071/MF17327>.

509

510 Lestrel, E. (Editor), 1997. Fourier Descriptors and their Application in Biology. Cambridge
511 University Press, London, UK.

512

513 Libungan, L. A., Palsson, S., 2015. ShapeR: an R package to study otolith shape variation
514 among fish populations. PLoS One 10. <https://doi.org/10.1371/journal.pone.0121102>.

515

516 Lombarte, A., Lleonart, J., 1993. Otolith size changes with body growth, habitat depth
517 and temperature. Environ. Biol. Fish. 37, 297-306.

518

519 Lunsford, D. R., Shotwell S. K., Hulson P-J. F., Hanselman, D. H., 2011. Assessment of the dusky
520 rockfish stock in the Gulf of Alaska. In Stock Assessment and Fishery Evaluation Report for the
521 Groundfish Resources of the Gulf of Alaska. North Pacific Fishery Management Council,
522 Anchorage, Alaska. <https://apps-afsc.fisheries.noaa.gov/REFM/docs/2011/GOAdusky.pdf>.

523

524 Mahé, K., Ider, D., Massaro, A., Hamed, O., Jurado-Ruzafa, A., Gonçalves, P., Anastasopoulou,
525 A., Jadau, A., Mytilineou, C., Elleboode, R., Ramdane, Z., Bacha, M., Amara, R., de Pontual, H.,
526 Ernande, B., 2019. Directional bilateral asymmetry in otolith morphology may affect fish stock

527 discrimination based on otolith shape analysis. ICES J. Mar. Sci. 76(1), 232-243.
528 doi:10.1093/icesjms/fsy163.

529

530 Malecha, P. W., Hanselman, D. H., Heifetz, J., 2007. Growth and mortality of rockfishes
531 (Scorpaenidae) from Alaska waters. U.S. Dep. Commer., NOAA Tech. Memo. NMFS-AFSC-172,
532 61 p.

533

534 Mapp, J., Hunter, E., Van, Der, Kooij, J., Songer, S., Fisher, M., 2017. Otolith shape and size: The
535 importance of age when determining indices for fish stock separation. Fish. Res. 190, 43-52.
536 doi:10.1016/j.fishres.2017.01.017.

537

538 Markowitz, E. H., Dawson, E. J., Charriere, N. E., Prohaska, B. K., Rohan, S. K., Stevenson, D. E.,
539 Britt, L. L., 2022. Results of the 2021 eastern and northern Bering Sea continental shelf bottom
540 trawl survey of groundfish and invertebrate fauna. U.S. Dep. Commer., NOAA Tech. Memo.
541 NMFS-AFSC-452, 227 p.

542

543 Mille, T., K. Mahé, M., Cachera, M., M. Villanueva, M. C., de Pontual, H., Ernande, B., 2016. Diet
544 is correlated with otolith shape in marine fish. Mar. Ecol. Prog. Ser. 555, 167-184. doi:
545 10.3354/meps11784.

546

547 Moralis-Nin, B., Pérez-Mayol, S., MacKenzie, K., Catalán, I. A., Palmer, M., Kersaudy, T., Mahé,
548 K., 2022. European hake (*Merluccius merluccius*) stock structure in the Mediterranean as

549 assessed by otolith shape and microchemistry. Fish. Res. 254, 106419.

550 <https://doi.org/10.1016/j.fishres.2022.106419>.

551

552 Moreira, C., Froufe, E., Vaz-Pires, P., Correia, A. T., 2019. Otolith shape analysis as a tool to infer
553 the population structure of the blue jack mackerel, *Trachurus picturatus*, in the NE Atlantic. J.

554 Fish. Res. 209, 40-48. <https://doi.org/10.1016/j.fishres.2018.09.010>.

555

556 Neves, J., Veríssimo, A., Santos, A. M., Garrido, S., 2023. Comparing otolith shape descriptors
557 for population structure inferences in a small pelagic fish, the European sardine *Sardina*
558 *pilchardus* (Walbaum, 1792). J. Fish. Biol. 102, 1219-1236. DOI: 10.1111/jfb.15369.

559

560 NPFMC (North Pacific Fishery Management Council), 2020a. The Fishery Management Plan for
561 Groundfish of the Bering Sea and Aleutian Islands Management Area.

562 <https://www.npfmc.org/wp-content/PDFdocuments/fmp/BSAI/BSAIfmp.pdf>.

563

564 NPFMC (North Pacific Fishery Management Council), 2020b. The Fishery Management Plan for

565 Groundfish of the Gulf of Alaska Management Area. <https://www.npfmc.org/wp->

566 [content/uploads/GOAfmmp.pdf](https://www.npfmc.org/wp-content/uploads/GOAfmmp.pdf).

567

568 Oksanen, J., Blanchet, F. G., Kindt, R., Legendre, P., Minchin, P.R., O'Hara, R.B., Solymos, P.,

569 Stevens, M., Szoecs, E., Wagner, H., Barbour, M., Bedward, M., Bolker, B., Borcard, D., Carvalho,

570 G., Chirico, M., De Caceres, M., Durand, S., Evangelista, H., FitzJohn, R., Friendly, M., Furneaux,

571 B., Hannigan, G., Hill, M., Lahti, L., McGlenn, D., Ouellette, M., Ribeiro Cunha, E., Smith, T., Stier,
572 A., Ter Braak, C., Weedon, J., 2013. vegan: Community Ecology Package, version 2.0–7. R
573 package. <http://CRAN.Rproject.org/package=vegan>.

574

575 Ortiz, I., Zador, S., 2021. Ecosystem status report 2021: Aleutian Islands, stock assessment and
576 fishery evaluation report. North Pacific Fishery Management Council, Anchorage, AK.

577

578 Park, J. M., Kang, M. G., Kim, J. H., Jawad, L. A., Majeed, S., 2023. Otolith morphology as a tool
579 for stock discrimination of three rockfish species in the East Sea of Korea. *Front. Mar. Sci.*
580 10:1301178. doi: 10.3389/fmars.2023.1301178.

581

582 Pebesma, E., 2018. Simple Features for R: Standardized Support for Spatial Vector Data. *The R*
583 *Journal* 10 (1), 439-446. <https://doi.org/10.32614/RJ-2018-009>.

584

585 Pebesma, E., Bivand, R., 2023. *Spatial Data Science: With Applications in R*. Chapman and
586 Hall/CRC. <https://doi.org/10.1201/9780429459016>.

587

588 R Core Team, 2022. *R: A Language and Environment for Statistical Computing*, Vienna, Austria.
589 Available from <<https://www.r-project.org/>>.

590

591

592

593 Rodgveller, C. J., Hutchinson, C. E., Harris, J. P., Vulstek, S. C., Guthrie, C. M., 2017. Otolith shape
594 variability and associated body growth differences in giant grenadier, *Albatrossia pectoralis*.
595 PLOS ONE 12(6), e0180020. <https://doi.org/10.1371/journal.pone.0180020>.
596
597 Sadighzadeh, Z., Tuset, V. M., Valinassab, T., Dadpour, M. R., Lombarte, A., 2012. Comparison of
598 different otolith shape descriptors and morphometrics for the identification of closely related
599 species of *Lutjanus* spp. from the Persian Gulf. Mar. Biol. Res 8, 802–814.
600 <http://dx.doi.org/10.1080/17451000.2012.692163>.
601
602 Smith, M. K., 1992. Regional differences in otolith morphology of the deep slope red snapper
603 *Etelis carbunculus*. Can. J. Fish. Aquat. Sci. 49, 795-804.
604
605 Smolinski, S., Schade, F. M., Berg, F., 2020. Assessing the performance of statistical classifiers to
606 discriminate fish stocks using Fourier analysis of otolith shape. Can. J. Fish. Aquat. Sci. 77, 674–
607 683. <http://dx.doi.org/10.1139/cjfas-2019-0251>.
608
609 Spencer, P., Canino, M., DiCosimo J., Dorn, M., Gharrett, A. J., Hanselman, D., Palof, K., M.
610 Sigler., 2010. Guidelines for determination of spatial management units for exploited
611 populations in Alaskan fishery groundfish management plans. Prepared for the September 2010
612 NPFMC Plan Team meeting. [https://www.npfmc.org/wp-](https://www.npfmc.org/wp-content/PDFdocuments/membership/PlanTeam/Groundfish/SpencerStockStructure0910.pdf)
613 [content/PDFdocuments/membership/PlanTeam/Groundfish/SpencerStockStructure0910.pdf](https://www.npfmc.org/wp-content/PDFdocuments/membership/PlanTeam/Groundfish/SpencerStockStructure0910.pdf).
614

615 Spencer, P. D., Ianelli, J. N., Laman, N., 2022. Assessment of blackspotted and rougheye
616 Rockfish stock complex in the Bering Sea/Aleutian Islands. In Stock Assessment and Fishery
617 Evaluation Report for the Groundfish Resources of the Bering Sea-Aleutian Islands. North Pacific
618 Fishery Management Council, Anchorage, Alaska. [https://apps-](https://apps-afsc.fisheries.noaa.gov/Plan_Team/2022/BSAIfrougheye.pdf)
619 [afsc.fisheries.noaa.gov/Plan_Team/2022/BSAIfrougheye.pdf](https://apps-afsc.fisheries.noaa.gov/Plan_Team/2022/BSAIfrougheye.pdf).

620

621 Stabeno, P.J., Bond, N.A., Hermann, A.J., Kachel, N.B., Mordy, C.W., Overland, J.E., 2004.
622 Meteorology and oceanography of the Northern Gulf of Alaska.
623 Cont. Shelf Res., 24, 859-897, 10.1016/j.csr.2004.02.007.

624

625 Stransky, C., 2005. Geographic variation of golden redfish (*Sebastes marinus*) and deep-sea
626 redfish (*S. mentella*) in the North Atlantic based on otolith shape analysis. ICES J. Mar. Sci. 62,
627 1691-1698. <https://doi.org/10.1016/j.icesjms.2005.05.012>.

628

629 Sullivan, J., Callahan M., Kingham A., TenBrink T., Ortiz I., Siddon E., Spencer, P., 2022.
630 Assessment of the Other Rockfish stock complex in the Bering Sea/Aleutian Islands. In Stock
631 Assessment and Fishery Evaluation Report for the Groundfish Resources of the Bering Sea-
632 Aleutian Islands. North Pacific Fishery Management Council, Anchorage, Alaska. [https://apps-](https://apps-afsc.fisheries.noaa.gov/Plan_Team/2022/BSAIfrock.pdf)
633 [afsc.fisheries.noaa.gov/Plan_Team/2022/BSAIfrock.pdf](https://apps-afsc.fisheries.noaa.gov/Plan_Team/2022/BSAIfrock.pdf).

634

635

636

637 TenBrink, T. T., Gburski, C. M., Hutchinson, C. E., 2023. Growth, distribution and mortality of
638 dusky rockfish and harlequin rockfish in the Aleutian Islands. *Mar. Coast. Fish.* 15(5), e10268.
639 DOI: 10.1002/mcf2.10268.
640
641 Tuset, V. M., Imondi, R., Aguado, G., Otero-Ferrer, J. L., Santschi, L., Lombarte, A., Love, M.,
642 2015. Otolith patterns of rockfishes from the northeastern Pacific. *J. Morphol.* 276, 458–469.
643 doi: 10.1002/jmor.20353.
644
645 Tuset, V. M., Otero-Ferrer, J. L., Siliprandi, C., Manjabacas, A., Marti-Puig, P., Lombarte, A.,
646 2021. Paradox of otolith shape indices: routine but overestimated use. *Can. J. Fish. Aquat. Sci.*
647 78, 681-692. <https://doi.org/10.1139/cjfas-2020-0369>.
648
649 Vaux, F., Rasmuson, L. K., Kautzi, L. A., Rankin, P. S., Blume, M. T. O., Lawrence, K. A., Bohn, S.,
650 O'Malley, K. G., 2019. Sex matters: Otolith shape and genomic variation in deacon rockfish
651 (*Sebastes diaconus*). *Ecol. Evol.* 9 (23), 13153-13173. DOI: 10.1002/ece3.5763.
652
653 Venables, W. N., Ripley, B. D., 2002. *Modern Applied Statistics with S*. Fourth Edition. Springer,
654 New York. ISBN 0-387-95457-0.
655
656 Vignon, M., Morat, F., 2010. Environmental and genetic determinant of otolith shape revealed
657 by a non-indigenous tropical fish. *Mar. Ecol. Prog. Ser.* 411, 231-241.
658

659 von Szalay, P. G., Raring, N. W., 2018. Data Report: 2017 Gulf of Alaska bottom trawl survey.
660 U.S. Dep. Commer., NOAA Tech. Memo. NMFS-AFSC-374, 260 p.
661

662 von Szalay, P. G., Raring, N. W., 2020. Data Report: 2018 Aleutian Islands bottom trawl survey.
663 U.S. Dep. Commer., NOAA Tech. Memo. NMFS-AFSC-409, 175 p.
664

665 Waite, J. N., Mueter, F. J., 2013. Spatial and temporal variability of chlorophyll-a concentrations
666 in the coastal Gulf of Alaska, 1998–2011, using cloud-free reconstructions of SeaWiFS and
667 MODIS-Aqua data. *Progr. Oceanogr.* 116, 179-192.
668 <https://doi.org/10.1016/j.pocean.2013.07.006>.
669

670 Waples, R. S., Punt, A. E., Cope, J. M., 2008. Integrating genetic data into management of
671 marine resources: how can we do it better? *Fish Fish.* 9(4), 423-449.
672

673 Wickham, H., 2016. *ggplot2: Elegant Graphics for Data Analysis*. Springer-Verlag New York. ISBN
674 978-3-319-24277-4, <https://ggplot2.tidyverse.org>.
675

676 Williams, B., Hulson, P-J. F., Lunsford, C. R., Ferriss, B., 2022. Assessment of the dusky rockfish
677 stock in the Gulf of Alaska. In *Stock Assessment and Fishery Evaluation Report for the*
678 *Groundfish Resources of the Gulf of Alaska*. North Pacific Fishery Management Council,
679 Anchorage, Alaska.
680 https://apps-afsc.fisheries.noaa.gov/Plan_Team/2022/GOAdusky.pdf.

681

682 Zhuang, L., Ye, Z., Zhang, C., 2015. Application of otolith shape analysis to species separation in
683 *Sebastes* spp. from the Bohai Sea and the Yellow Sea, northwest Pacific. Environ. Biol. Fish. 98,
684 547–558. doi: 10.1007/s10641-014-0286-z.

685

686 Zimmermann, M., Prescott, M. M., 2021. Passes of the Aleutian Islands: First detailed
687 description. Fish. Oceanogr. 30(3), 280-299. <https://doi.org/10.1111/fog.12519>.

688

689

690

691

692

693

694

695

696

697

698

699

700

701

702

703 **Table 1.** Otolith collections of dusky rockfish (*Sebastes variabilis*) by management region,
 704 subarea, sample sizes (*n*) of otolith side, and years of sampling used in this study.

| Region | Subarea | Statistical Area | <i>n</i> | | Year(s) |
|--------|--------------------------|------------------|----------|------|------------------------|
| | | | Right | Left | |
| BSAI | Eastern Aleutian Islands | 541 | 51 | 64 | 2019, 2020, 2021 |
| | Central Aleutian Islands | 542 | 26 | 41 | 2019, 2020, 2021 |
| | Western Aleutian Islands | 543 | | 42 | 2019, 2020, 2021, 2022 |
| GOA | Western Gulf of Alaska | 610, 620,630 | 112 | 117 | 2019, 2020, 2021 |
| | Eastern Gulf of Alaska | 640, 650 | 37 | 32 | 2019, 2021 |
| Total | | | 226 | 296 | |

705

706

707

708

709

710

711

712

713

714

715

716

717 **Table 2.** Shape indices calculated for dusky rockfish (*Sebastes variabilis*) otoliths. F_L = Feret
 718 length; F_W = Feret width; O_A = otolith area; O_{AC} = otolith convex hull area; O_P = otolith
 719 perimeter.

| Shape index | Formula |
|----------------|-----------------------------|
| Aspect ratio | F_L / F_W |
| Circularity | O_P^2 / O_A |
| Ellipticity | $(F_L - F_W) / (F_L + F_W)$ |
| Form factor | $4\pi O_A / O_P^2$ |
| Rectangularity | $O_A / (F_L \times F_W)$ |
| Roundness | $(4O_A) / (\pi F_L^2)$ |

720

721

722

723

724

725

726

727

728

729 **Table 3.** Summary table for non-parametric Kruskal–Wallis tests of the null hypothesis that each
 730 size or shape index from each otolith side is identical between five subareas of the Bering Sea
 731 and Aleutian Islands and Gulf of Alaska. The Kruskal-Wallis test statistic (H) approximates a Chi-
 732 square distribution. Eta squared (η^2) effect values followed Cohen (1988): 0.01 – 0.06 (small
 733 effect), 0.06 – 0.14 (moderate effect) and > 0.14 (large effect). Note: List includes indices that
 734 exhibited either a large or a moderate effect.

| Variable | Otolith side | $H (X^2)$ | Eta Squared (η^2) |
|----------------|--------------|-----------|--------------------------|
| Area | Right | 40.4 | 0.168 |
| Otolith length | Right | 32.6 | 0.133 |
| Otolith weight | Right | 34.0 | 0.139 |
| Area | Left | 31.5 | 0.094 |
| Otolith length | Left | 31.6 | 0.094 |
| Otolith width | Left | 25.7 | 0.075 |
| Roundness | Left | 54.1 | 0.172 |
| Otolith weight | Left | 29.6 | 0.088 |

735
 736
 737
 738
 739
 740
 741
 742
 743

744 **Table 4.** ANOVA-like permutation tests from standardized wavelet and elliptic Fourier
 745 coefficients. df = degrees of freedom; SS = sum of squares; F = F value.

| Otolith | Descriptor | | df | SS | F | P -value |
|------------|------------|----------|-----|--------|------|------------|
| Left-side | Fourier | Model | 4 | 0.09 | 4.04 | 0.001 |
| | | Residual | 291 | 1.56 | | |
| | Wavelet | Model | 4 | 12.53 | 5.11 | 0.001 |
| | | Residual | 291 | 178.19 | | |
| Right-side | Fourier | Model | 3 | 0.05 | 3.01 | 0.001 |
| | | Residual | 222 | 1.30 | | |
| | Wavelet | Model | 3 | 6.03 | 2.55 | 0.001 |
| | | Residual | 222 | 175.97 | | |

746

747

748

749

750

751

752

753

754

755

756

757 **Table 5.** Results of PERMANOVA testing for differences in otolith shape between subareas for
 758 left and right-side otoliths.

| | | WAI | CAI | EAI | EGOA | WGOA |
|-------|---------|----------------------------------|-------|-------|-------|-------|
| Left | WA | | 0.26 | 1 | 0.145 | 0.005 |
| | CAI | | | 0.803 | 0.012 | 0.001 |
| | EAI | | | | 0.015 | 0.001 |
| | EGOA | | | | | 1 |
| | WGOA | | | | | |
| | Fourier | Psuedo $F = 4.125$; $P < 0.001$ | | | | |
| | WA | | 0.672 | 0.435 | 0.009 | 0.001 |
| | CAI | | | 1 | 0.001 | 0.001 |
| | EAI | | | | 0.001 | 0.001 |
| | EGOA | | | | | 0.966 |
| Right | CAI | | | 0.984 | 0.007 | 0.030 |
| | EAI | | | | 0.005 | 0.234 |
| | EGOA | | | | | 1 |
| | Wavelet | Psuedo $F = 4.654$; $P < 0.001$ | | | | |

WGOA

Fourier Psuedo $F = 2.946$; $P < 0.001$

CAI 1 0.022 0.016

EAI 0.001 0.002

EGOA 0.523

WGOA

Wavelet Psuedo $F = 2.883$; $P < 0.001$

759

760

761

762

763

764

765

766

767

768

769

770

771

772

773 **Figure captions (color for publication)**

774 Figure 1. Map of the study area showing sampling locations and corresponding subareas within
775 the BSAI (WAI = 541, CAI = 542, EAI = 543) and Gulf of Alaska management regions (WGOA =
776 610, 620, 630; EGOA = 640, 650). Dashed line corresponds to the line of separation between
777 management regions.

778

779 Figure 2. Example of a left-side otolith used in this study (A); and its corresponding ShapeR
780 otolith reconstruction outline (b). Scale bar = 1 mm.

781

782 Figure 3. Size and shape indices from otolith analysis of dusky rockfish (*Sebastes variabilis*)
783 within subareas of the Bering Sea and Aleutian Islands (blue) and Gulf of Alaska management
784 regions (orange). Box plots show the median and inter-quartile (IQR) range, maximum and
785 minimum values ($\pm 1.5 \times \text{IQR}$), mean (closed circles) and outliers (open circles).

786

787 Figure 4. Mean otolith shape of dusky rockfish (*Sebastes variabilis*) based on wavelet
788 reconstruction for each subarea for the left-side otolith (top) and right-side otolith (bottom).

789

790 Figure 5. Canonical analysis of principal coordinates (CAP) plot of otolith shapes from
791 standardized wavelet and elliptic Fourier coefficients. Labeled subareas represent the mean
792 canonical coordinates surrounded by two standard errors (SEs).

793

794

795 Figure 6. Classification matrix of the linear discriminant analysis (LDA) for subarea classification
796 of dusky rockfish (*Sebastes variabilis*) based on best performing model for left and right-side
797 otoliths. The cell values indicate the number of otoliths classified by subarea, with correctly
798 classified percentages in the highlighted cells. Shading represents the percent of otoliths
799 classified by observed subarea, with higher classification rates in green.

800

801

802

803

804

805

806

807

808

809

810

811

812

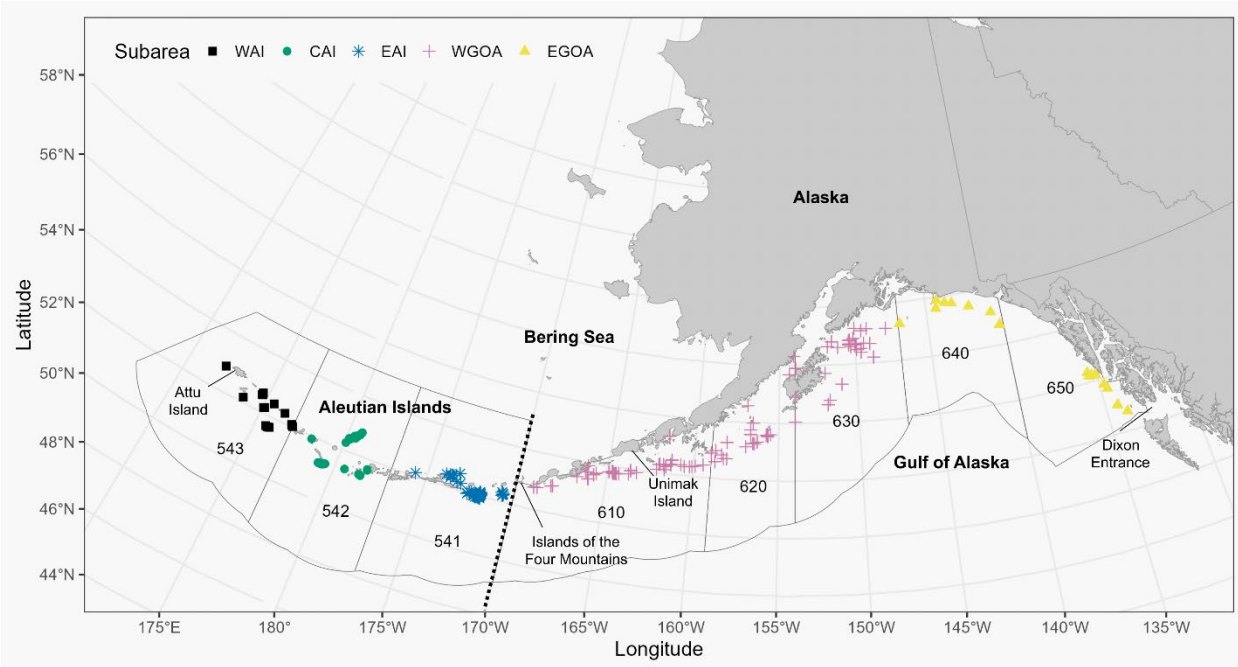
813

814

815

816

817 **Figure 1.**



818

819

820

821

822

823

824

825

826

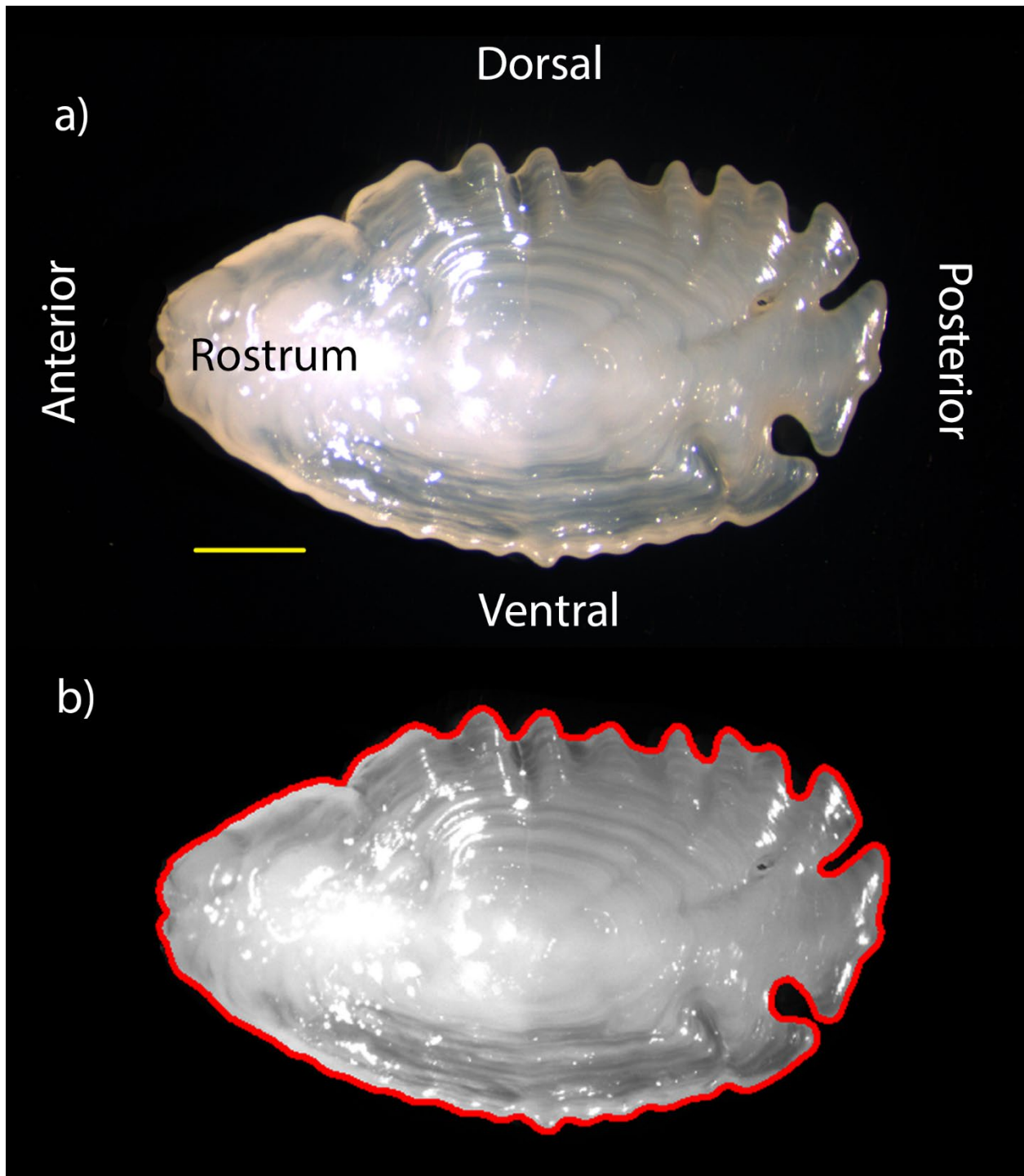
827

828

829

830

831 Figure 2.

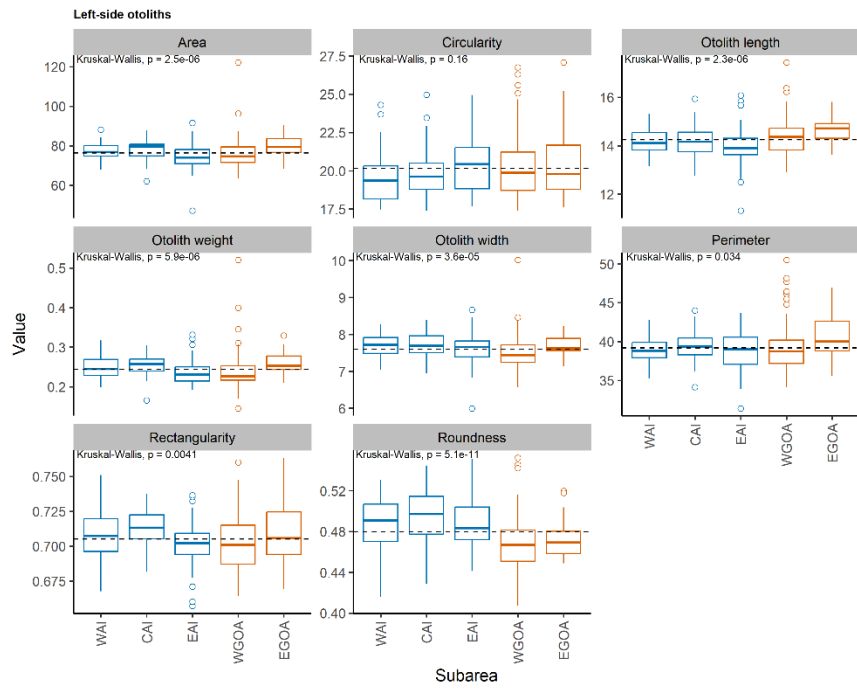


832

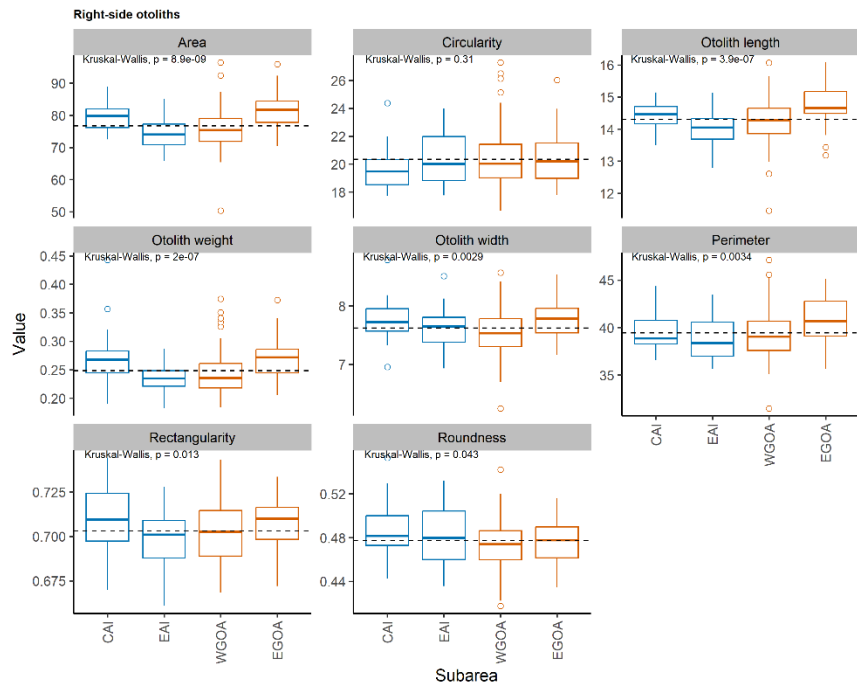
833

834

835 **Figure 3.**



836



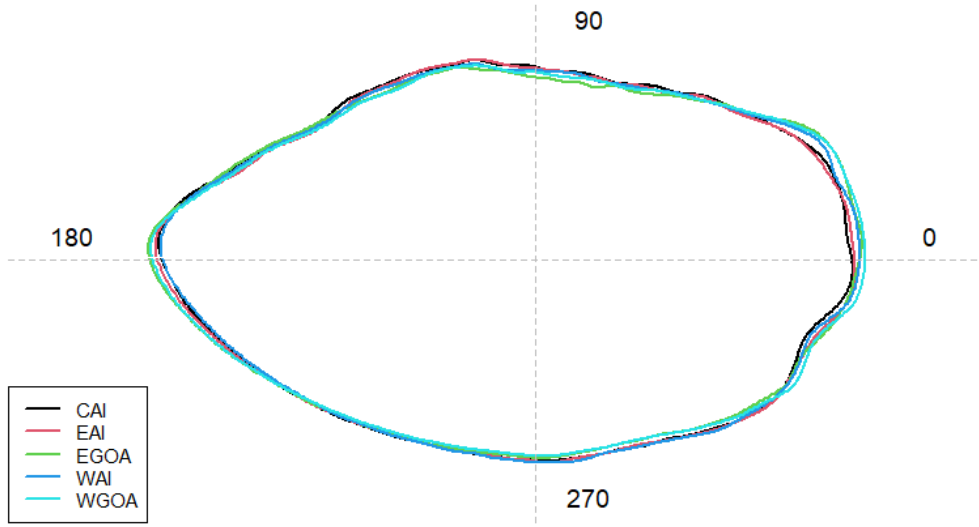
837

838

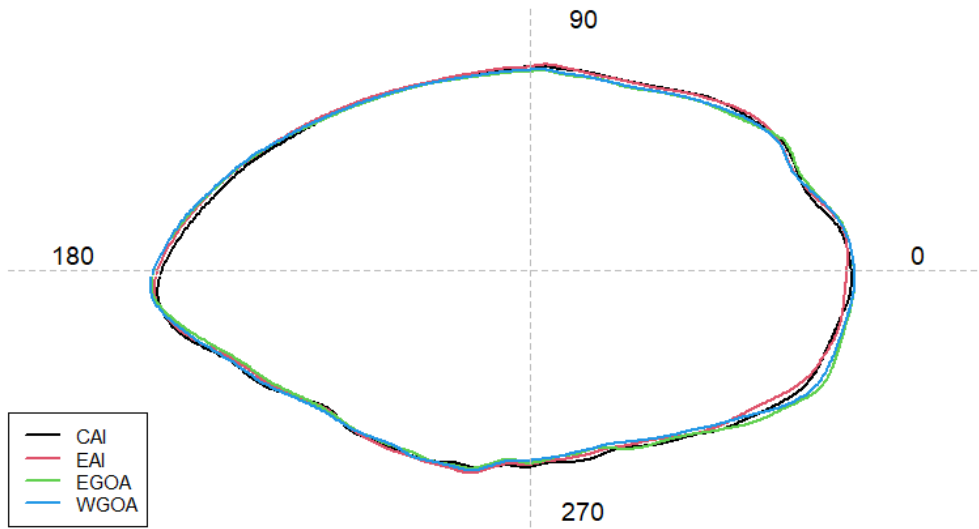
839

840

841 Figure 4.



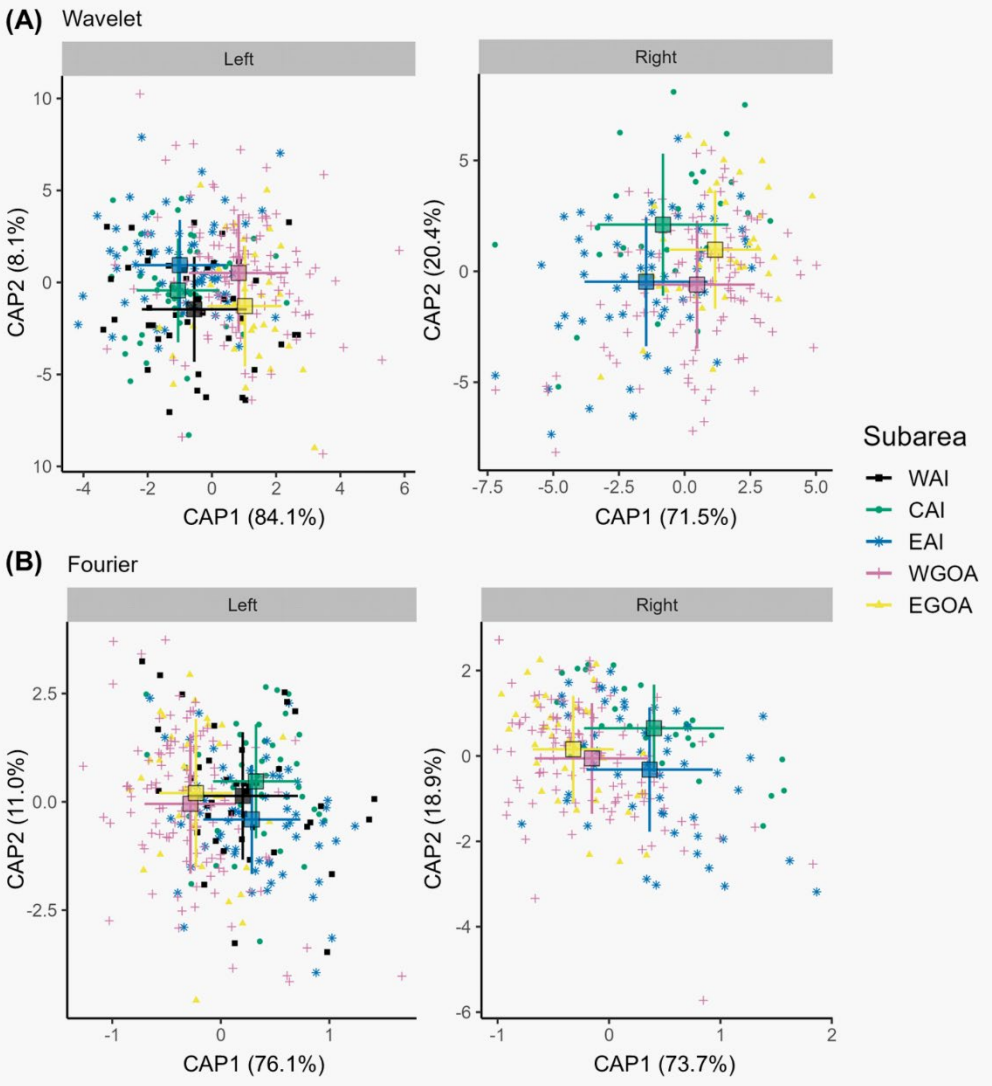
842



843

844

845 **Figure 5.**



846

847

848

849

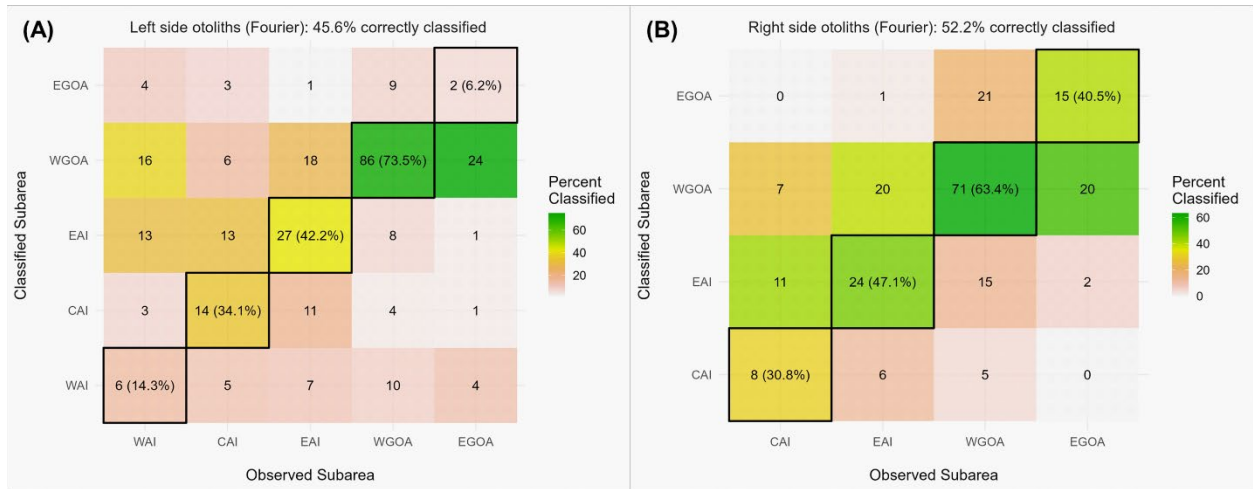
850

851

852

853

854 **Figure 6.**



855

856

857

858

859

860

861

862

863

864

865

866

867